

An Experimental Study and a Thermodynamic Evaluation of the Fe-Mo-W System

Per Gustafson

(Division of Physical Metallurgy, The Royal Institute of Technology, S-10044 Stockholm, Sweden)

An experimental study of the Fe-Mo-W system has been made using a diffusion couple technique. A number of tie-lines have been determined using a scanning electron microscope with an energy dispersive X-ray analysis equipment. A thermodynamic evaluation has been made using a magnetic subregular model for the bcc and fcc solution phases, a multi-sublattice model for the intermetallic phases and an ordinary subregular solution model for the liquid phase. A set of parameter values describing the Gibbs energy of each individual phase is given and a number of calculated sections of the Fe-Mo-W phase diagram are presented and compared with experimental data.

Experimentelle Untersuchung und thermodynamische Optimierung des Systems Fe-Mo-W

Das System Fe-Mo-W wurde experimentell mit Hilfe von Diffusionspaaren untersucht. Einige Konoden wurden experimentell durch Raster-Elektronen-Mikroskopie mit energiedispersiver Röntgenanalyse bestimmt. Das System wurde thermodynamisch optimiert, wobei für die krz und kfz Phase ein Untergittermodell mit Zusatztermen für Magnetismus, für die intermetallischen Phasen ein Modell mit mehreren Untergittern und für die Schmelze eine normale subreguläre Beschreibung gewählt wurde. Ein Satz Parameter zur Berechnung der freien Enthalpie jeder Phase wird angegeben. Das System Fe-Mo-W wird durch eine Anzahl berechneter Schnitte dargestellt und diese mit experimentellen Daten verglichen.

1 Introduction

Available experimental information in the ternary Fe-Mo-W system is very sparse. In a recent review by Raynor et al.¹) only one modern examination of the constitution of the ternary system was found. Kirchner et al.²) determined a number of tie-lines on the bcc/bcc + μ and the bcc/bcc + R phase boundaries at 1373 and 1578 K using electron microprobe analysis on ternary alloys prepared from high purity materials.

In the present paper results from a new experimental investigation will be presented together with an evaluation of the thermodynamic properties of the system. The purpose of the experimental part of the present work was to obtain a more complete picture of the system. The experimental work was thus focused on regions of the phase diagram not investigated by Kirchner et al. In the present work tie-lines have been determined at 1473, 1573 and 1673 K using several diffusion couples.

A scanning electron microscope, JEOL JSM-840, equipped with an energy dispersive X-ray spectrometer (EDS) and LINK AN10000 X-ray microanalysis system was used to determine the phase interface compositions. Thanks to the simultaneous use of a secondary electron detector and a backscatter electron detector it was easy to place the electron beam at exact positions.

2 Experimental

Binary Fe-Mo, Fe-W and Mo-W alloys were prepared from pure elements by arc melting of compacts obtained from powders. The composition of the raw materials are presented in Table 1 and the compositions of the alloys are presented in Table 2.

The diffusion couples were prepared by taking a solid piece of iron and drilling a hole into it and inserting coin-shaped pieces of the other two components or binary

alloys into the hole and finally pressing a rod of pure iron into the hole while the solid piece was supported from the side. Finally the solid piece was compressed locally perpendicular to the interface between the interfaces the coin-shaped pieces in order to ascertain good contact. The compound specimen was sealed in a silica

Table 1. The compositions of the raw materials used in the preparation of the binary alloys.

Material	Impurity contents in wt.%			
Capsule:	< 0.01 Cr	0.006 C	0.001 Si	
	0.019 Mn	0.003 P	0.011 S	
	< 0.031 (Ni + Mo + Cu + Sn + Co)	rest Fe		
Electrolytic Iron	0.003 Al	< 0.003 Mn	< 0.005 S	
	0.01 C	0.001 Si	0.002 N	
Mo	99.9 Mo	0.004 C	0.006 S	
W	99.95 W	0.031 C		

Table 2. The compositions and designation of the binary alloys, the pure metals and the capsule material used in the present work.

Alloy designation	Composition in wt.%		
	Fe	Mo	W
Capsule	Bal.	< 0.03	-
25 Mo	75	25	-
60 Mo	40	60	-
80 Mo	20	80	-
Mo	0.01	Bal.	0.002
50 W	50	-	50
90 W	10	-	90
W	< 0.02	< 0.02	Bal.
Mo 5 W	-	95	5
Mo 10 W	-	90	10
Mo 15 W	-	85	15
Mo 25 W	-	75	25
Mo 50 W	-	50	50

capsule under vacuum and heat treated during the times given in Table 3. The temperature was controlled to within ± 5 K. After the given time, the specimen was quenched in brine. The cylindrical specimen was cut parallel to the center-line of the initial hole, mounted in electrically conductive bakelite and prepared metallographically.

The compositions of various phases appearing at the interfaces were studied with an EDS analyzer. Several measurements were taken along lines perpendicular to phase interfaces and the compositions of coexisting phases were evaluated by extrapolation to the position of their interface. Local equilibrium was then assumed to hold at the boundaries and the associated compositions were taken as defining tie-lines. All tie-lines determined in the present work are presented in Table 4.

In systems, where the differences in diffusion rates are small, it is often possible to cover a whole section with only one compound specimen just by combining pieces of the pure components. This was not possible in the present work. The reason was that iron diffused into the interface between the two other components and separated them. As a result only binary Fe-Mo and Fe-W tie-lines were obtained with this kind of specimen configuration. The diffusion couple technique thus had to be slightly modified. The specimens were composed of binary alloys in addition to the pure components. Diffusion couples prepared from binary Mo-W alloys and pure iron proved very useful.

Table 3. The constitution of the various compound specimens and information on heat treatments performed.

Compound specimen		Temp. (K)	Time (h)
Designation	Constitution		
M1	60 Mo 90 W 80 Mo	1473 \pm 5	100
M2	W Mo 50 W Mo 25 W Mo	1703 \pm 10	6
M3	W Mo 50 W 25 Mo Mo 25 W	1473 \pm 5	72
M4	50 W Mo 50 W Mo 25 W Mo	1573 \pm 5	47
M5	Mo W 80 Mo	1581 \pm 5	310
M6	50 W 60 Mo 90 W Mo	1673 \pm 5	28
M7	Mo Mo Mo 50 W 60 Mo 50 W Mo Mo	1673 \pm 5	164
M8	Mo 25 W Mo 15 W Mo 10 W Mo 5 W 80 Mo	1673 \pm 5	72

The three intermetallic phases R, μ and σ are all stable close to the binary Fe-Mo side of the ternary system at the temperatures of investigation. They formed as parallel layers at the compound interfaces. Some of them could be very thin and it was not always possible to get reliable results from the measurements. In some cases the R phase did not precipitate at all. For example only σ phase was found at the interface between the two components in binary Fe-Mo diffusion couples heat treated at 1673 K. Figure 1 shows a secondary electron image of the diffusion zone close to the interface after 72 h of annealing and Fig. 2 shows the corresponding concentration profile measured along the line perpendicular to the phase interfaces indicated in Fig. 1. The profile presented in Fig. 2 shows no sign of the expected R/ σ two-phase equilibrium and the homogeneity range measured for the σ phase widely extends the homogeneity range found in the stable system³. At first sight this result may seem confusing but a closer examination of the accepted properties of the binary Fe-Mo system reveals that the R phase is very close to being metastable in this system and the σ phase will

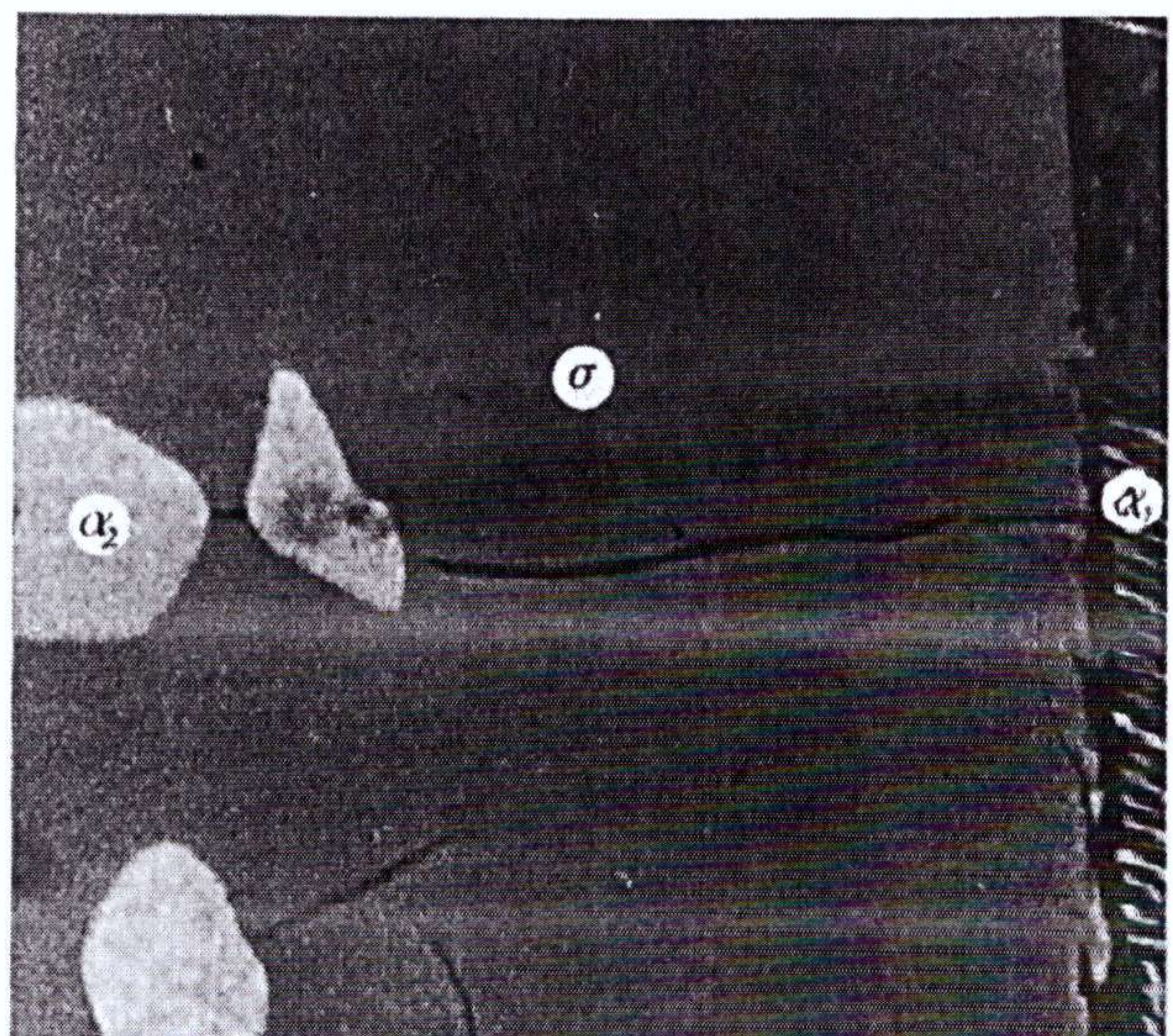


Fig. 1. A secondary electron image of the diffusion zone in alloy M8 (80 Mo/Fe) equilibrated at 1673 K for 72 h.

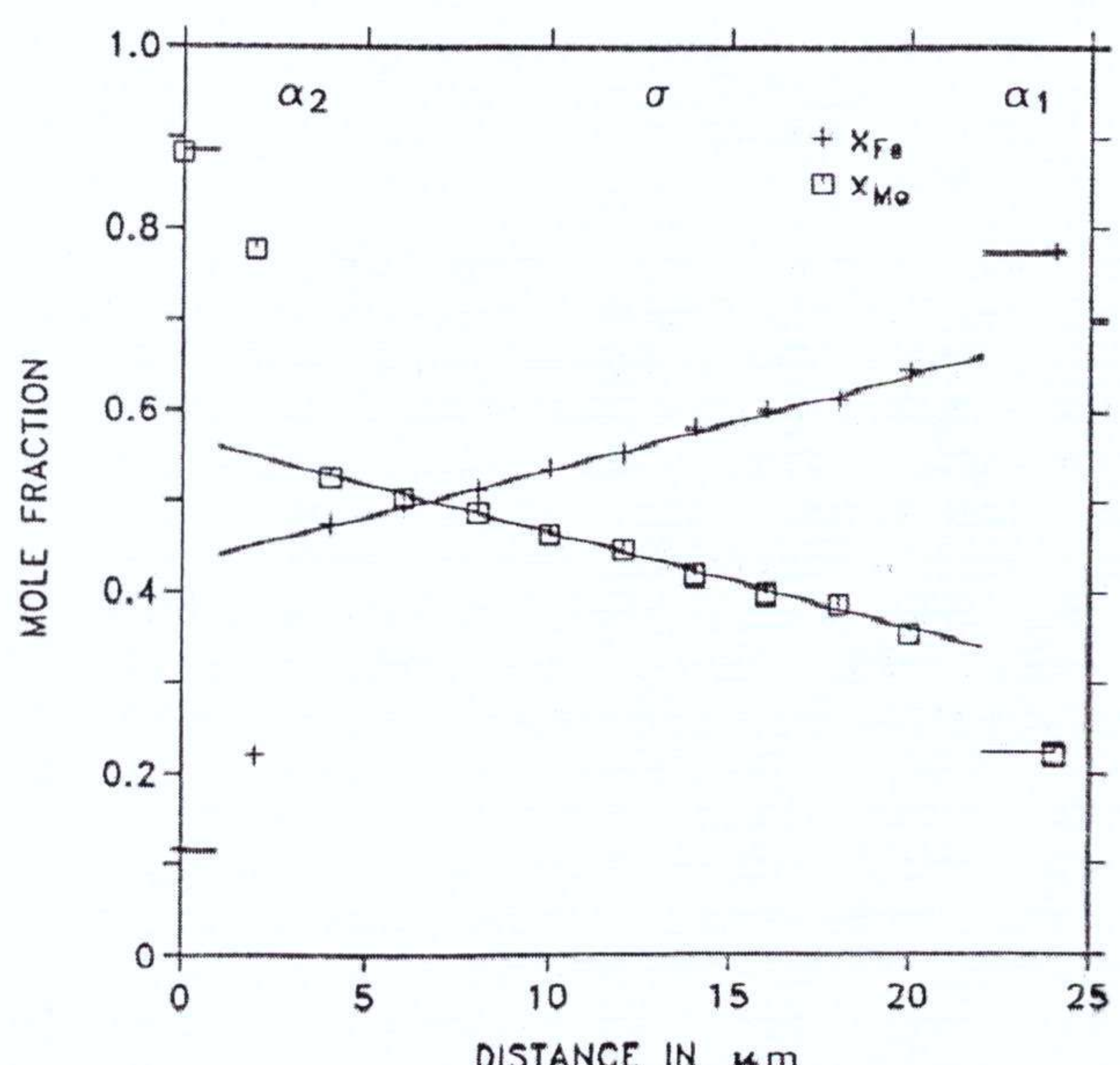


Fig. 2. The molybdenum and iron concentration profiles across the bcc and sigma phases indicated in Fig. 1.

Table 4. Experimental tie-lines. Compositions are expressed in mole fractions. The stars (*) indicate that the given phase takes part in the equilibrium but its composition was not determined.

From specimen	Tie-line designation	Phases P.1/P.2	Phase 1		Phase 2		Comments
			Mo	W	Mo	W	
M1	1M2	bcc/ μ	0.120	0.008	0.370	0.020	
	1M1	bcc/ μ	0.084	0.025	0.300	0.080	
	1M3	μ /bcc	0.432	0.005	0.940	0.006	
	1M4	μ /bcc	0.428	0.020	0.925	0.020	
M3	3M1	bcc/ μ	0.100	0.020	0.300	0.077	
	3M2	μ /bcc	0.360	0.075	0.808	0.150	
	3M3	bcc/ μ	0.062	0.032	0.208	0.192	
	3M5	μ /bcc	0.268	0.175	0.565	0.425	
M4	4M1-1	μ / σ	0.436	0.000	0.546	0.000	
	4M1-2	σ /bcc	0.569	0.000	0.920	0.000	
	4M2	μ /bcc	0.378	0.070	0.826	0.124	
	4M3	μ /bcc	0.300	0.150	0.590	0.400	
M5	5M1	bcc/ μ	0.073	0.042	0.165	0.230	
	5M2	μ /bcc	0.027	0.430	0.030	0.955	
	5M4-1	μ / σ	0.440	0.000	0.542	0.000	
	5M4-2	σ /bcc	0.569	0.000	0.927	0.000	
M6	6M6	σ /bcc	0.57	0.000	0.895	0.000	
	6M8	bcc/ σ	0.223	0.000	0.335	0.000	
	6M10	bcc/ μ	0.125	0.045	0.220	0.186	
	6M12	bcc/R	0.160	0.030	0.280	0.078	
M7	6M13	bcc/	0.195	0.015	*	*	R or σ
	7M3	bcc/ μ	0.025	0.084	0.045	0.370	
	7M4	bcc/ μ	0.078	0.066	0.174	0.226	
	7M5	bcc/ μ	0.082	0.066	0.180	0.212	
	7M6	bcc/ μ	0.050	0.076	0.110	0.290	
	7M7	μ /bcc	0.268	0.190	0.561	0.388	
	7M10	bcc/ μ	0.108	0.053	0.212	0.188	
	7M13	μ /bcc	0.255	0.190	0.570	0.380	
	7M14	μ /bcc	0.260	0.184	0.563	0.386	
		μ /bcc	0.262	0.196	0.522	0.420	
		μ /bcc	0.253	0.195	0.511	0.430	
		μ /bcc	*	*	0.304	0.047	R or σ
		μ /	0.312	0.065	0.340	0.065	R or σ
M8	8M2-1	bcc/	*	*	0.420	0.068	
	8M2-2	μ /	0.367	0.068	0.420	0.068	
	8M2-3	μ / σ	0.470	0.075	0.775	0.136	
	8M2-4	σ /bcc	0.380	0.046	0.426	0.053	
	8M3-1	μ / σ	0.500	0.053	0.820	0.093	
	8M3-2	σ /bcc	0.401	0.043	0.429	0.048	
	8M5	μ / σ	0.345	0.056	0.353	0.055	R or σ
	8M6	μ /	0.535	0.018	0.887	0.028	
	8M8	σ /bcc	0.565	0.001	0.885	0.000	
	8M9	σ /bcc	0.309	0.059	0.324	0.065	R or σ
	8M21-1	μ /	0.348	0.067	0.418	0.065	
	8M21-2	μ / σ	0.383	0.041	0.416	0.042	
	8M22	μ / σ	0.395	0.028	0.425	0.030	
	8M24	μ / σ	0.570	0.000	*	*	

form in a much wider composition range if no R phase nucleates. Figure 3 shows the binary Fe-Mo phase diagram as calculated by Fernandez Guillerm⁴⁾ and Fig. 4 shows the corresponding metastable Fe-Mo phase diagram calculated after suspending the R phase. The agreement with the experimental tie-lines in Fig. 4 is very good. This result can serve as a good example of how a thermodynamic calculation in some cases can facilitate the interpretation of experimental data. The nucleation difficulties found for the R phase made the interpretation of some of the ternary data very difficult. The μ phase in the ternary system separates the iron and the molybdenum rich parts of the σ phase and it was thus not always possible to distinguish between the stable bcc/R and the metastable bcc/ σ equilibrium or the stable R/ μ and the metastable σ / μ equilibrium. In order to distinguish between the various possibilities an X-ray structure analysis at the interfaces must be made. This could not be done within the present work. Apart from the above mentioned difficulties, the experi-

mental data obtained in the present work gives a very good picture of the constitution of the ternary system in the temperature range 1473 to 1673 K. The experimental tie-lines are also in very good agreement with the data given by Kirchner et al.²⁾ in those regions where a comparison can be made.

3 Thermodynamic Models

A model describing the thermodynamic properties of phases with several sublattices which was recently developed⁵⁾ will be applied in the present work. The model can also handle a contribution to the Gibbs energy due to magnetic ordering in the form suggested by Inden⁶⁾ and Hillert and Jarl⁷⁾. The Curie or Neel temperature and the average magnetic moment per atom must be given as functions of composition.

3.1 fcc, bcc and Liquid Phases

For the bcc, fcc and liquid phases a subregular solution model was chosen. The model yields the following expression for the Gibbs energy,

$$G_m = x_{Fe} {}^0G_{Fe}^h + x_{Mo} {}^0G_{Mo}^h + x_W {}^0G_W^h + RT(x_{Fe} \ln x_{Fe} + x_{Mo} \ln x_{Mo} + x_W \ln x_W) + G_m^E + G_m^{mo} \quad (1)$$

where

$$G_m^E = x_{Fe} x_{Mo} L_{Fe,Mo} + x_{Fe} x_W L_{Fe,W} + x_{Mo} x_W L_{Mo,W} + x_{Fe} x_{Mo} x_W L_{Fe,Mo,W} \quad (2)$$

The three binary L parameters can be concentration dependent according to a Redlich-Kister polynomial. The parameter ${}^0G_i^h$ is the Gibbs energy of pure component i in a hypothetical non-magnetic state. All the 0G values are given relative to the enthalpy of selected reference states for the elements at 298.15 K. This state is denoted by SER (Stable Element Reference). The term G_m^{mo} represents the contribution due to magnetic ordering. The magnetic term is only needed in the Gibbs energy expression for the bcc phase. For the fcc phase it is negligible except for very low temperatures and it may thus be neglected for the present purpose. The parameter ${}^0G_{Fe}^h$ is then identical to the Gibbs energy of real fcc Fe. For such phases the superscript h will be omitted.

3.2 Intermetallic Phases

The binary intermetallic phases in the Fe-Mo system have been modeled by Fernandez Guillermet³). He gives a detailed description of how the crystal structure of each phase can be taken into account. Andersson and Sundman⁸) applied the same technique to the Fe-Cr σ phase but modified the number of sites on individual sublattices to be able to account for the high molybdenum contents found in the ternary Cr-Fe-Mo σ phase⁹). Their modification also made it possible to account for the high chromium and molybdenum contents found in ternary Cr-Ci-W and Cr-Ni-Mo σ phases^{10,11}). This slightly adjusted model was recently adopted by Fernandez Guillermet⁴) in a revision of the Fe-Mo system. The binary intermetallic phases in the Fe-W system have been modeled by Andersson and Gustafson¹²). Their description was later revised by Gustafson¹³) in order to conform with the accepted description of the pure elements. The σ and R phases are not stable in the binary Fe-W system. Even though not stable, it is reasonable to believe that they should be considered as metastable. The ternary model was thus obtained from the binary model presented by Fernandez Guillermet, simply by allowing W to substitute for Mo on all sites allowed for Mo. The σ , R and μ phases are described with the three-sublattice model through the formulas $(Fe)_8(Mo,W)_4(Fe,Mo,W)_{18}$, $(Fe)_{27}(Mo,W)_{14}(Fe,Mo,W)_{12}$ and $(Fe)_7(Mo,W)_2(Fe,Mo,W)_4$, respectively. The sublattice model yields the following expression for the Gibbs energy for a mole of formula units,

$$\begin{aligned} G_m = & {}^2y_{Mo} ({}^3y_{Fe} {}^0G_{Fe:Mo:Fe} + {}^3y_{Mo} {}^0G_{Fe:Mo:Mo} + {}^3y_W {}^0G_{Fe:Mo:W}) + \\ & {}^2y_W ({}^3y_{Fe} {}^0G_{Fe:W:Fe} + {}^3y_{Mo} {}^0G_{Fe:W:Mo} + {}^3y_W {}^0G_{Fe:W:W}) + \\ & aRT ({}^2y_{Mo} \ln {}^2y_{Mo} + {}^2y_W \ln {}^2y_W) + \\ & bRT ({}^3y_{Fe} \ln {}^3y_{Fe} + {}^3y_{Mo} \ln {}^3y_{Mo} + {}^3y_W \ln {}^3y_W) + \\ & {}^2y_{Mo} ({}^3y_{Fe} {}^3y_{Mo} L_{Fe:Mo:Fe,Mo} + {}^3y_{Fe} {}^3y_W L_{Fe:Mo:Fe,W} + {}^3y_{Mo} {}^3y_W L_{Fe:Mo:Mo,W}) + \\ & {}^2y_W ({}^3y_{Fe} {}^3y_{Mo} L_{Fe:W:Fe,Mo} + {}^3y_{Fe} {}^3y_W L_{Fe:W:Fe,W} + {}^3y_{Mo} {}^3y_W L_{Fe:W:Mo,W}) \end{aligned} \quad (3)$$

The notations 2y_i and 3y_i refer to the site fractions of the component i in the second and third sublattice, respectively. The number of sites, denoted by a and b , are 4 and 18 for the σ phase, 14 and 12 for the R phase and 2 and 4 for the μ phase. The 0G parameters for the intermetallic phases are given relative to the selected reference state

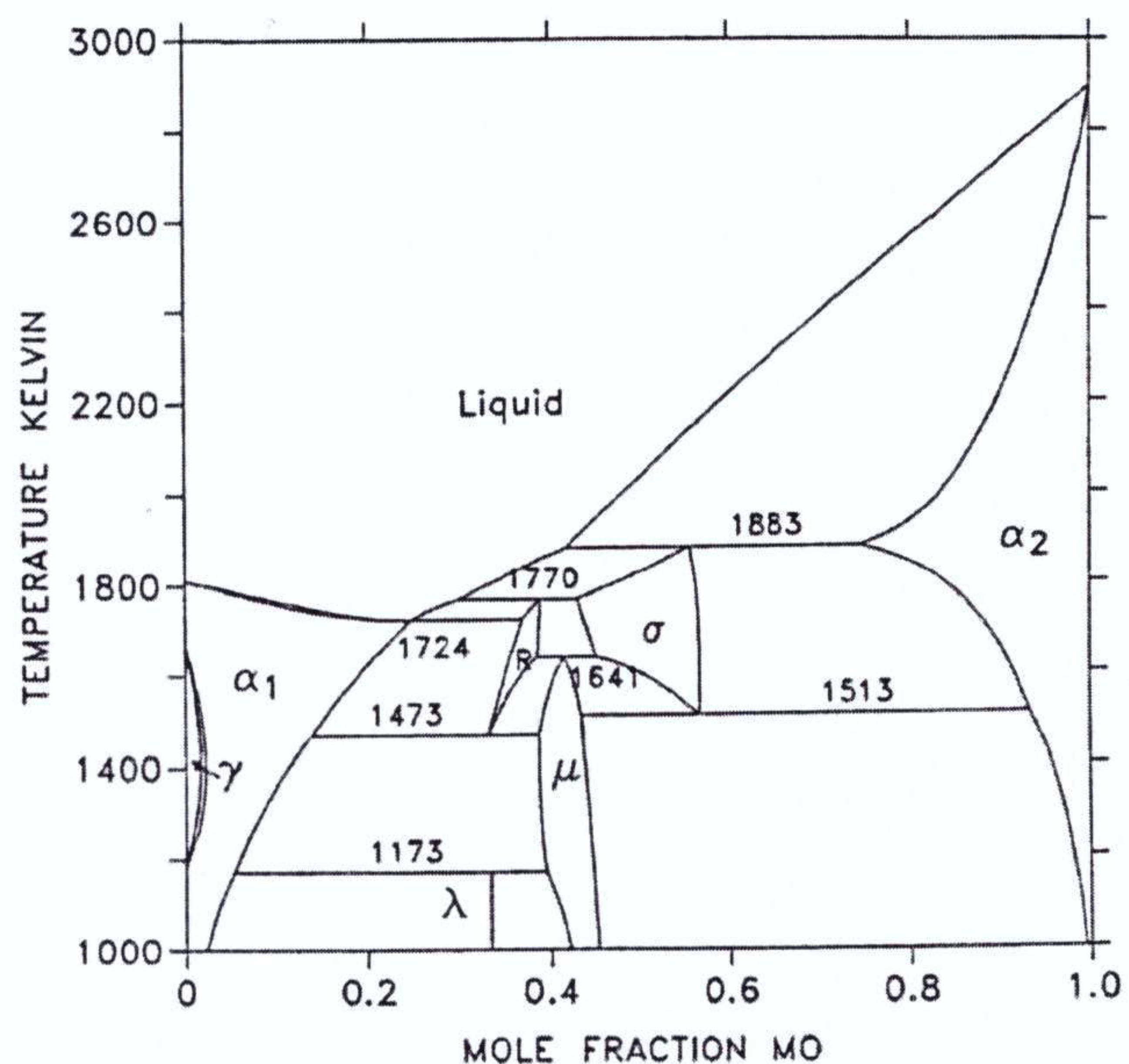


Fig. 3. The complete Fe-Mo phase diagram according to the present description. α and γ are used to denote the bcc and fcc phases.

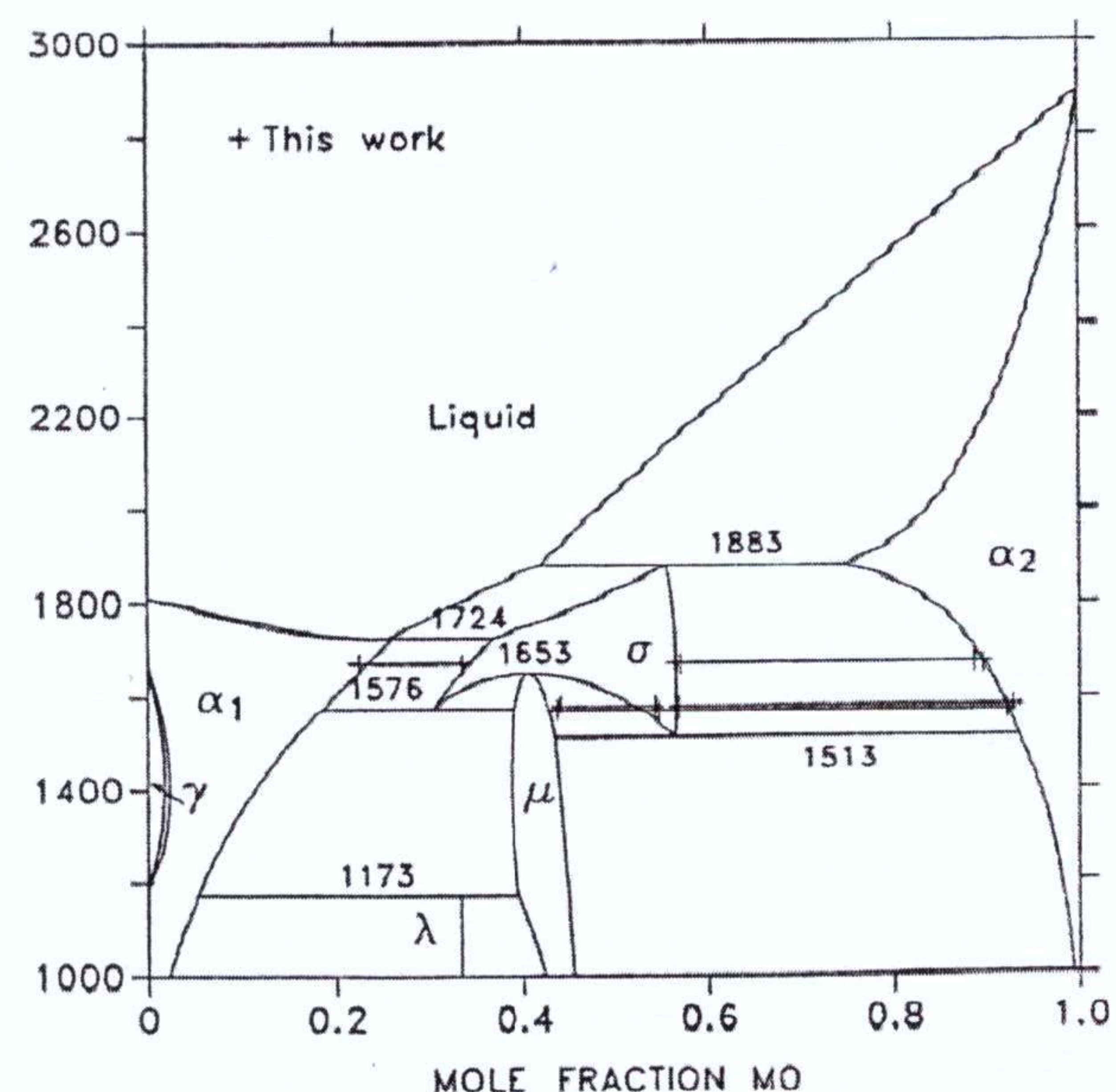


Fig. 4. The metastable Fe-Mo phase diagram, calculated by suspending the R phase, in comparison with experimental tie-lines.

for the elements. Andersson et al.¹⁴⁾ suggested that the ${}^{\circ}G$ quantities could as a first approximation be estimated by comparing the atoms in the different sublattices with bcc and fcc structures. Atoms on sublattices with 12 neighbors (CN12) could be compared with fcc atoms and atoms on sublattices with CN14 and higher with bcc atoms. The predictions given by this approach when experimental data are lacking are hopefully reasonable but in cases when experimental data are available an additional correction term is often needed. In the present evaluation a fairly small constant value had to be used in most cases.

The thermodynamic properties of the metastable binary phases had to be estimated from ternary data. The properties of binary Fe-W σ phase were estimated in a parallel study of the Cr-Fe-W system¹⁵⁾ by the present author. The properties of binary Fe-W R phase were estimated from Kirchner's data and the data obtained in this work.

The Laves phase is stable in the binary Fe-Mo and Fe-W systems at low temperatures^{3) 12) 13)}. The ternary model $(\text{Fe})_2(\text{Mo}, \text{W})_1$ will be used. However, very little is known about the behaviour of this phase in the ternary system.

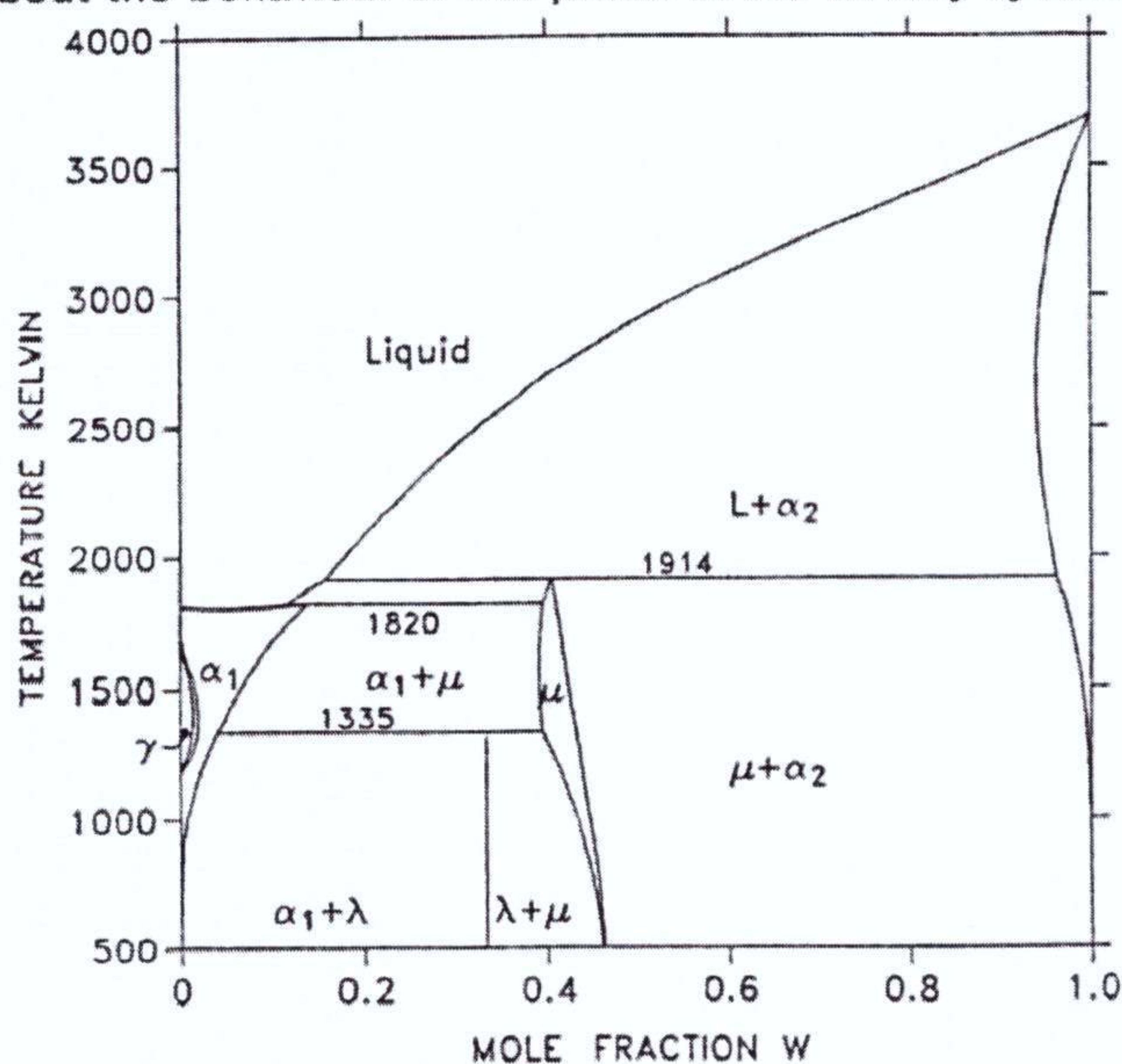


Fig. 5. The complete Fe-W phase diagram according to the present description.

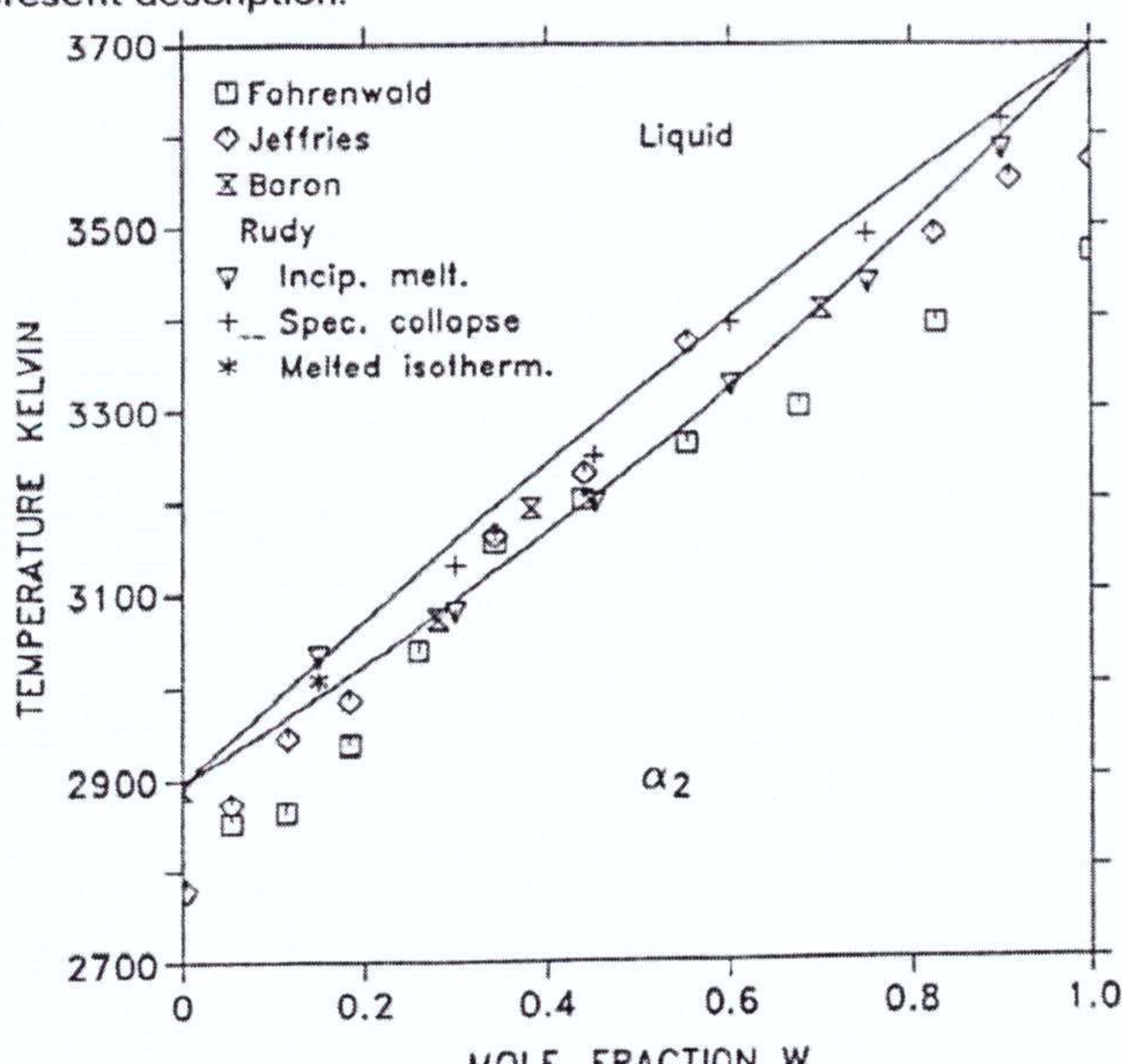


Fig. 6. The Mo-W phase diagram according to the present evaluation.

4 Evaluation of the Phase Diagram

The thermodynamic descriptions of the elements and the binary Fe-Mo and Fe-W systems have been evaluated prior to the present work. The thermodynamic properties of Fe, Mo and W have been evaluated by Fernandez Guillermet and Gustafson¹⁶⁾, Fernandez Guillermet¹⁷⁾ and Gustafson¹⁸⁾, respectively. The binary Fe-Mo has been analysed by Fernandez Guillermet^{3) 4)}, the binary Fe-W by Gustafson¹³⁾. The calculated binary Fe-Mo and Fe-W phase diagrams are reproduced in Figs. 3 and 5.

The evaluation of the various parameters was made by means of a computer program for the optimization of thermodynamic parameters developed by Jansson^{19) 20)}. First the binary Mo-W system was considered. This system has recently been reviewed by Nagender Naidu et al.²¹⁾. Available experimental data show that it is close to ideal. Kaufman et al.²²⁾ and Brewer et al.²³⁾ estimated the interaction energies in the bcc and liquid phases by considering internal pressure and size differences. These effects indicate a small positive deviation from ideality. The interaction energy in the liquid given by Kaufman corresponds to a regular solution parameter close to 5300 J/mol. Brewer also used a subregular parameter but without giving any reason. The internal pressure contribution is described in terms of the solubility parameters for binary partners. The solubility parameters are defined as,²²⁾

$$d_{\text{Mo}} = (-H_{\text{Mo}}/V_{\text{Mo}})^{1/2} \text{ and } d_{\text{W}} = (-H_{\text{W}}/V_{\text{W}})^{1/2},$$

where H_{Mo} and H_{W} are the enthalpy of vaporization and V_{Mo} and V_{W} the molar volume. The internal pressure contribution is evaluated by squaring the difference between d_{Mo} and d_{W} and multiplying with the average molar volume. Both, Kaufman and Brewer, based their computations on room temperature values and their estimates must be regarded as very approximate. Instead of using Kaufman's or Brewer's interaction energies, it was decided to put the regular solution parameter in the liquid to zero. The dominating contribution in their interaction energy for the bcc phase originated from internal pressure. Instead of using their values, the L parameter was evaluated from the experimental liquid/bcc data quoted in Ref.²¹⁾. The calculated phase diagram is shown in Fig. 6 together with the experimental data.

The results of the optimization of ternary data are presented and compared with experimental data in Figs. 7 to 12. Since the μ phase is the dominating phase in the ternary system it was first investigated how the bcc 1/ μ and μ /bcc 2 equilibria could best be described. A set of representative tie-lines from the work by Kirchner et al. and from the present work were selected for optimization. First the bcc and μ phases were assumed to have no ternary interactions and only the two ${}^{\circ}G$ parameters were considered. Temperature independent values for the optimized correction terms were found to give a fairly good description of the phase boundaries. However, the calculated μ /bcc 2 tie-lines were still not quite satisfactory. In order to improve on this a ternary interaction in the bcc had to be introduced. A small value gave a slight improvement but still the calculated iron solubility in the Mo and W rich bcc phase seemed too high, in particular at low temperatures. No further attempt was made to improve the fit, partly because it was felt that the discrepancy may be due to experimental errors. The diffusion of iron into the interior of the binary Mo-W specimens was very slow, perhaps even negligible, since the μ /bcc phase boundary moved in the

same direction as the iron diffusion. The experimental technique sets the limit on how close to the phase boundary the composition can be determined accurately to roughly $2 \mu\text{m}$. In view of this it is not surprising that the experimental iron solubilities were so low.

The next step was to consider the σ phase. In order to describe the binary Fe-Mo σ phase, Fernandez Guillermet⁴) needed a fairly large interaction parameter in addition to the two $^{\circ}\text{G}$ parameters. In the ternary model his parameter corresponds to a positive interaction between Fe and Mo on the third sublattice when there is only Mo on the second sublattice. However, for simplicity it was now assumed that the interaction between Fe and Mo is independent of the content on the second sublattice. This assumption gives, $L_{\text{Fe}:W:\text{Fe},\text{Mo}} = L_{\text{Fe}:W:\text{Mo},\text{Fe}} = 22909 \text{ J/mol}$. The binary Fe-W σ phase has been considered by the pres-

ent author in connection to a parallel evaluation of the ternary Cr-Fe-W system¹⁵). The binary Fe-W σ phase is described with two $^{\circ}\text{G}$ parameters and a positive interaction parameter.

The sublattice model for the σ phase gives two additional $^{\circ}\text{G}$ parameters and a number of interaction parameters to be evaluated in the ternary system. The experimental data obtained in the present work were not sufficient for an evaluation of all of them and some assumptions had to be made. First it was assumed that all interactions between Mo and W are equal to zero, and that $L_{\text{Fe}:W:\text{Fe},\text{W}}$ is equal to $L_{\text{Fe}:W:\text{W},\text{Fe}}$ which was estimated in the parallel study¹⁵). When optimizing the two remaining parameters, $^{\circ}\text{G}_{\text{Fe}:W:\text{Mo}}$ and $^{\circ}\text{G}_{\text{Fe}:W:\text{W}}$, it was found that $^{\circ}\text{G}_{\text{Fe}:W:\text{Mo}}$ could not be unambiguously determined. As a result $^{\circ}\text{G}_{\text{Fe}:W:\text{Mo}}$ could just as well be given an arbitrary value. It was put equal to.

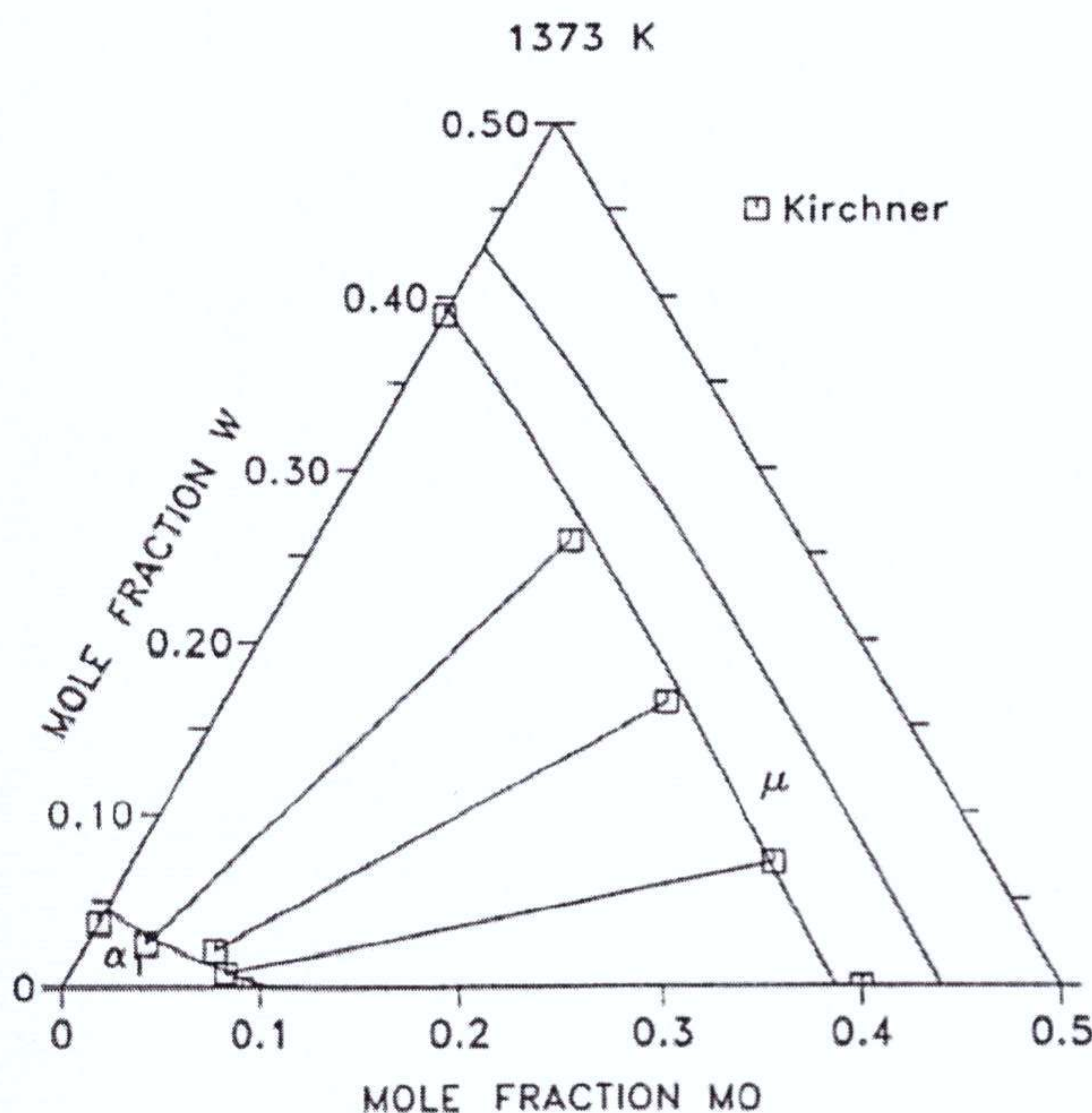


Fig. 7. The calculated isothermal section of the Fe-Mo-W system at 1373 K in comparison with experimental data.

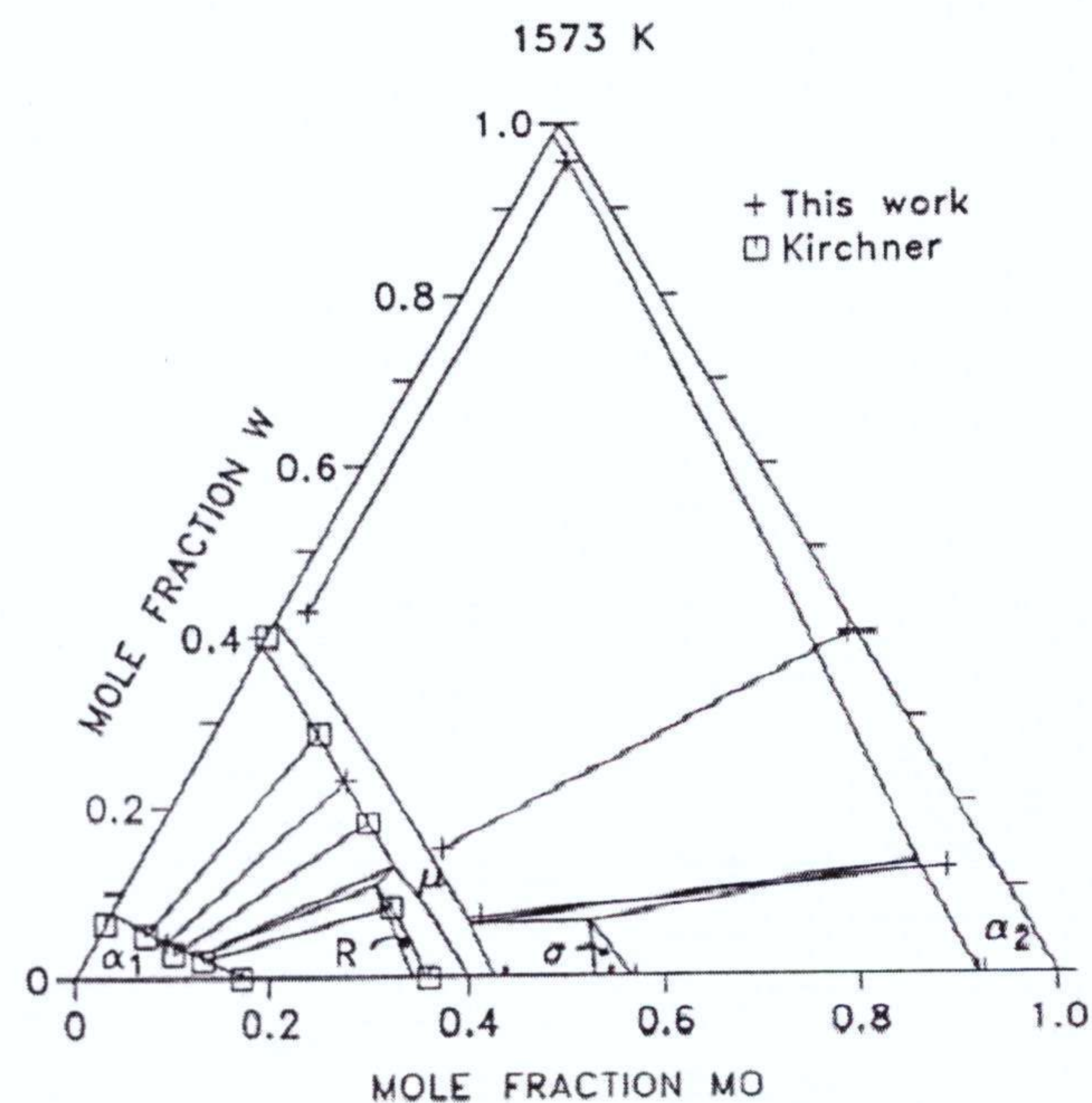


Fig. 9. The calculated isothermal section of the Fe-Mo-W system at 1573 K in comparison with experimental data.

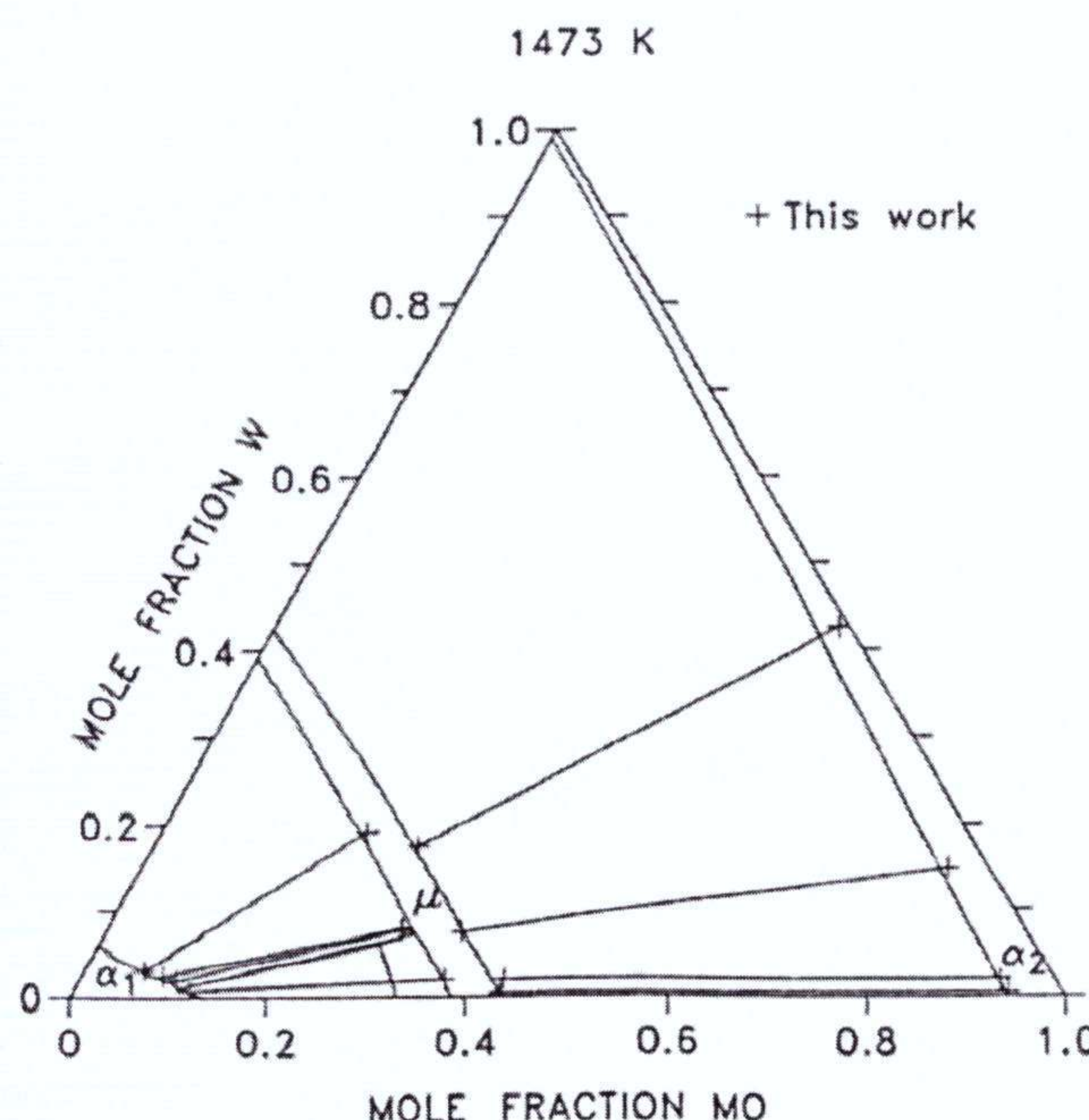


Fig. 8. The calculated isothermal section of the Fe-Mo-W system at 1473 K in comparison with experimental data.

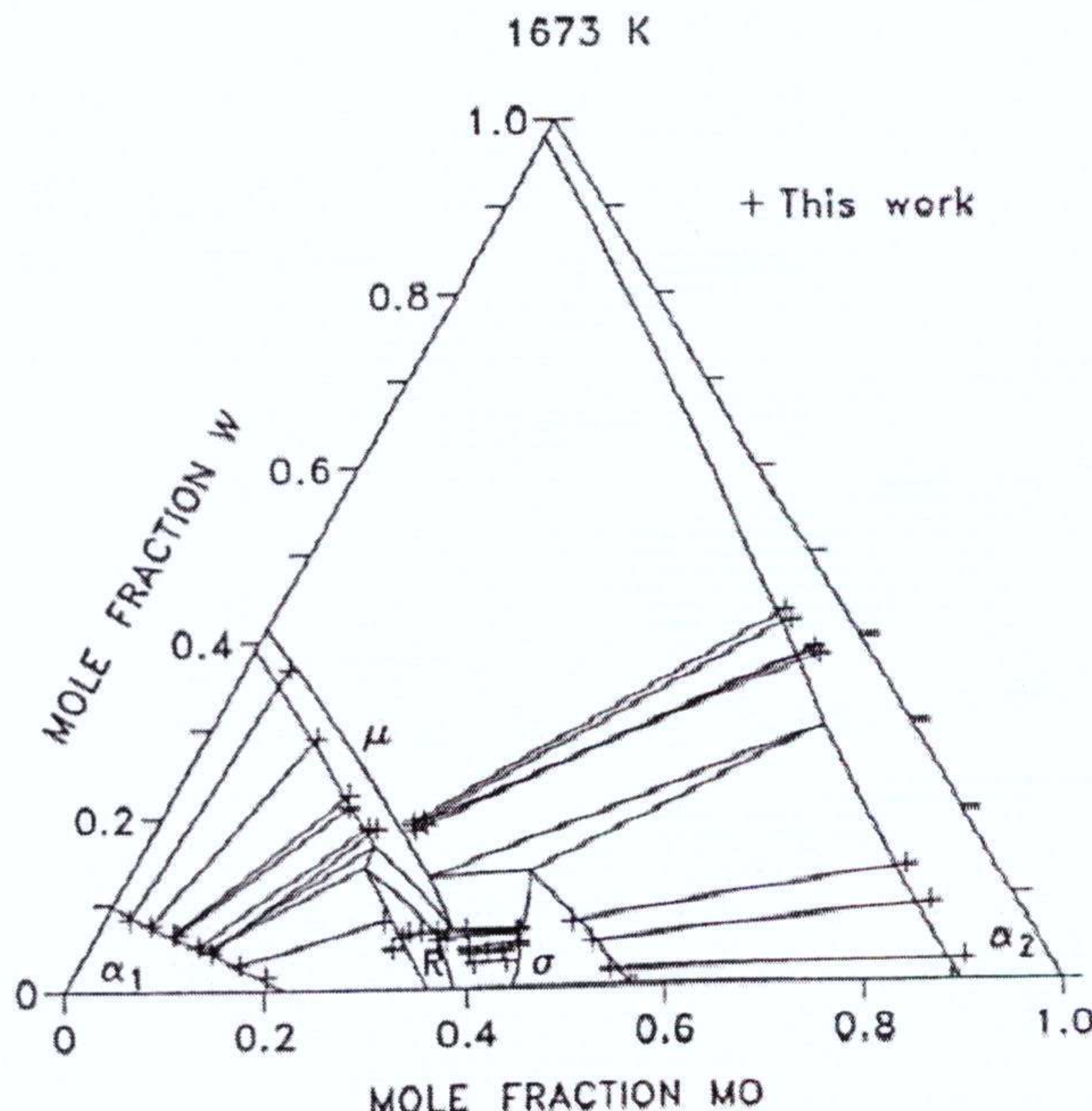


Fig. 10. The calculated isothermal section of the Fe-Mo-W system at 1673 K in comparison with experimental data.

$$^{\circ}G_{Fe:W:Mo} = 8 \cdot ^{\circ}G_{Fe}^{bcc} + 4 \cdot ^{\circ}G_W^{bcc} + 18 \cdot ^{\circ}G_{Mo}^{bcc}$$

Only one parameter thus remained to be optimized, $^{\circ}G_{Fe:Mo:W}$, that parameter alone could account for all experimental data.

Finally the R phase was introduced. The experimental knowledge concerning this phase is still very sparse. In the ternary system only the bcc/R tie-line by Kirchner et al. is certain. The interpretation of the experimental tie-lines at 1673 K are somewhat uncertain, as discussed previously. The optimization was conducted with Kirchner's value at 1581 K and the tie-lines designated 6M12, 8M6 and 8M21-1 in Table 4. Only one parameter could be evaluated from this limited set of data. The description must be considered provisional, even though the agreement with the selected data is satisfactory.

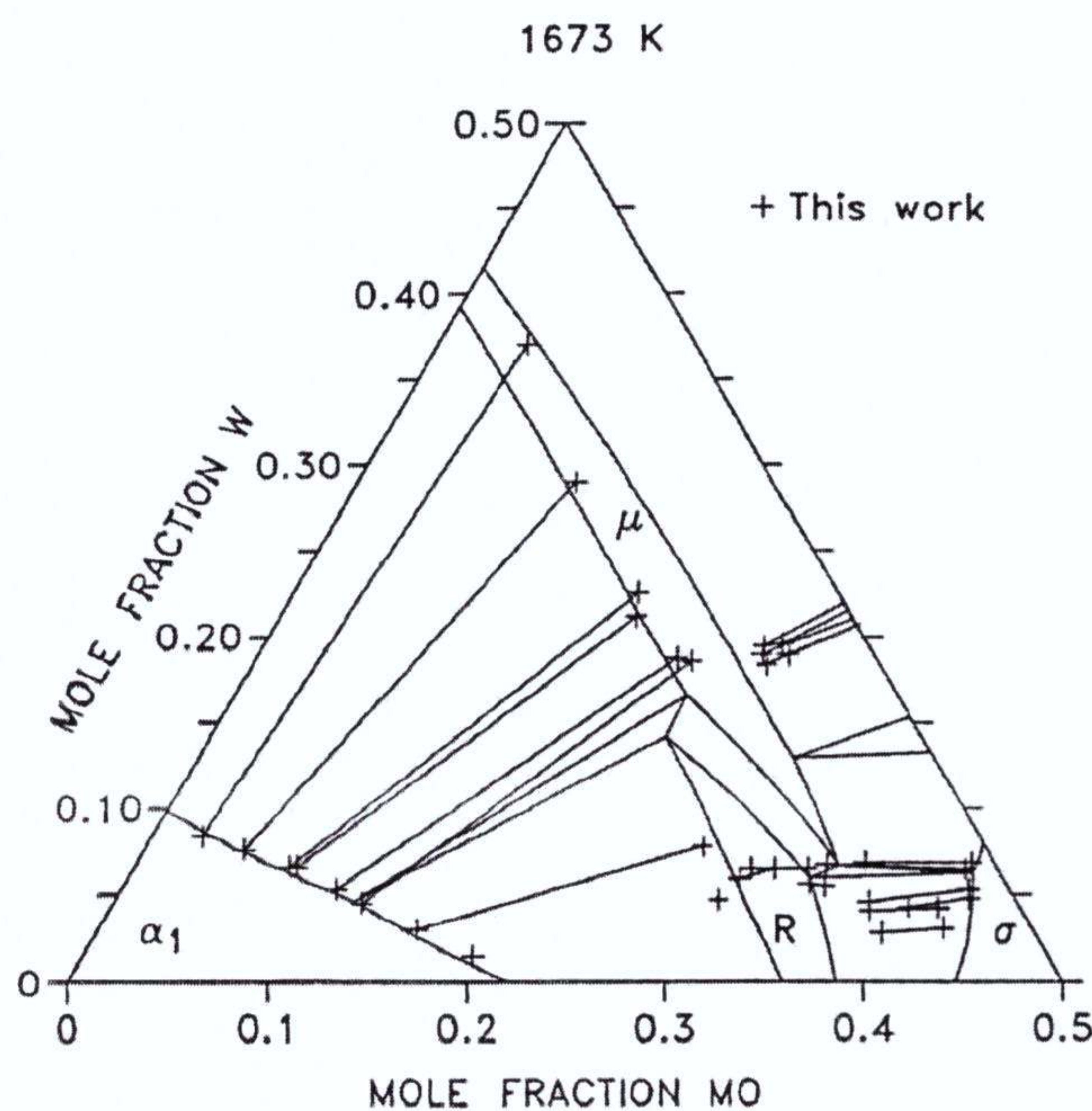


Fig. 11. Part of the calculated isothermal section of the Fe-Mo-W system at 1673 K in comparison with experimental data.

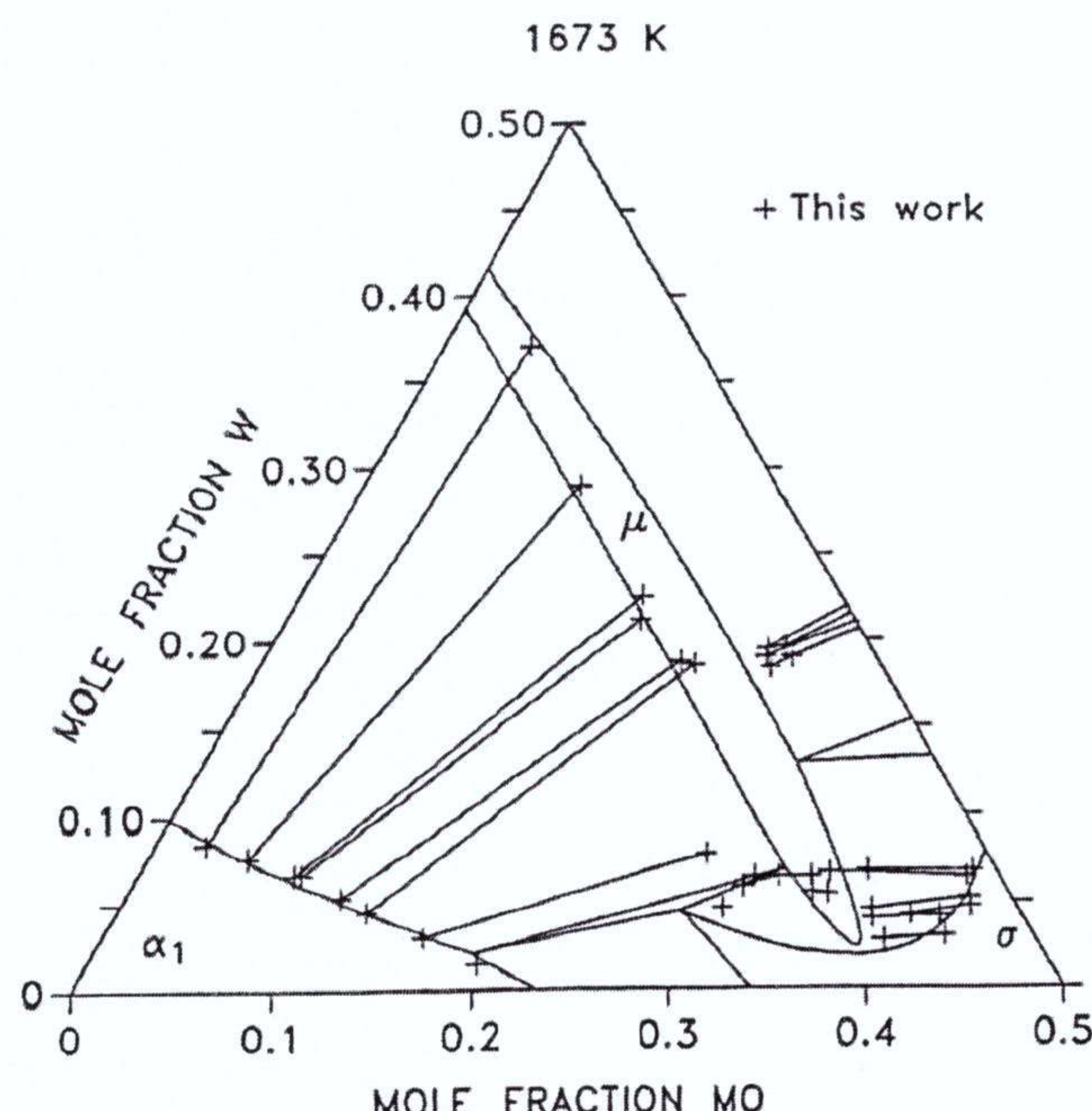


Fig. 12. Part of the metastable isothermal section at 1673 K, calculated by suspending the R phase, in comparison with experimental data.

In order to obtain the best possible agreement, all selected data were used simultaneously in a final optimization. Figures 7 to 12 show a number of isothermal sections calculated with the final set of parameters. As can be seen in these figures the final description represents most experimental data well within the experimental uncertainties. Figure 11 shows the calculated iron rich corner at 1673 K. The scatter in the experimental data makes it difficult to improve the description further. Figure 12 shows the corresponding metastable section calculated after suspending the R phase. Comparing Figs. 11 and 12 it is seen that some data seem to be better represented by Fig. 12 than Fig. 11 and they may thus hold for metastable equilibria.

Most of the experimental data discussed in the present paper are limited to the temperature region 1373 to 1700 K.

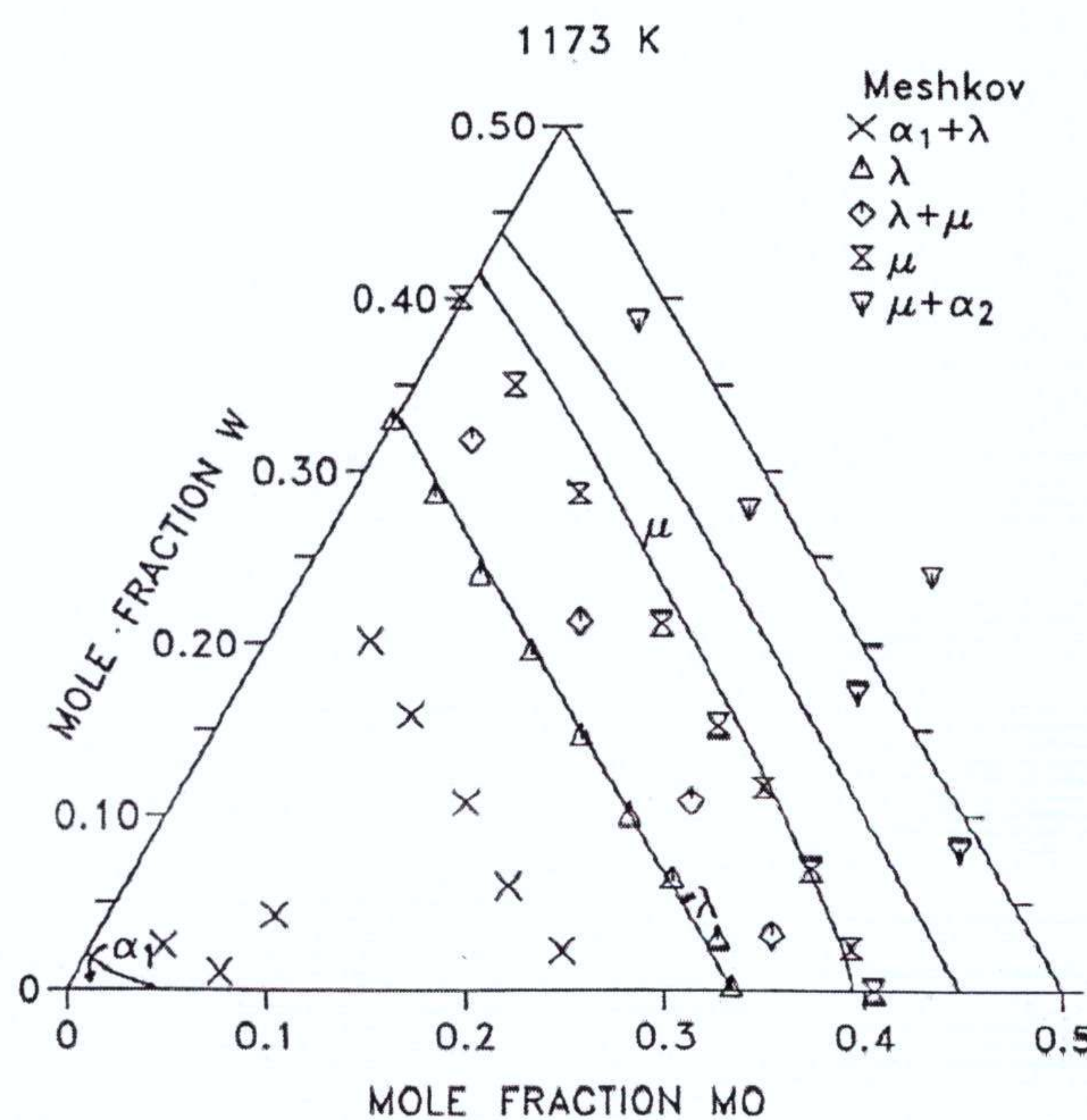


Fig. 13. The calculated isothermal section of the Fe-Mo-W system at 1173 K in comparison with experimental data.

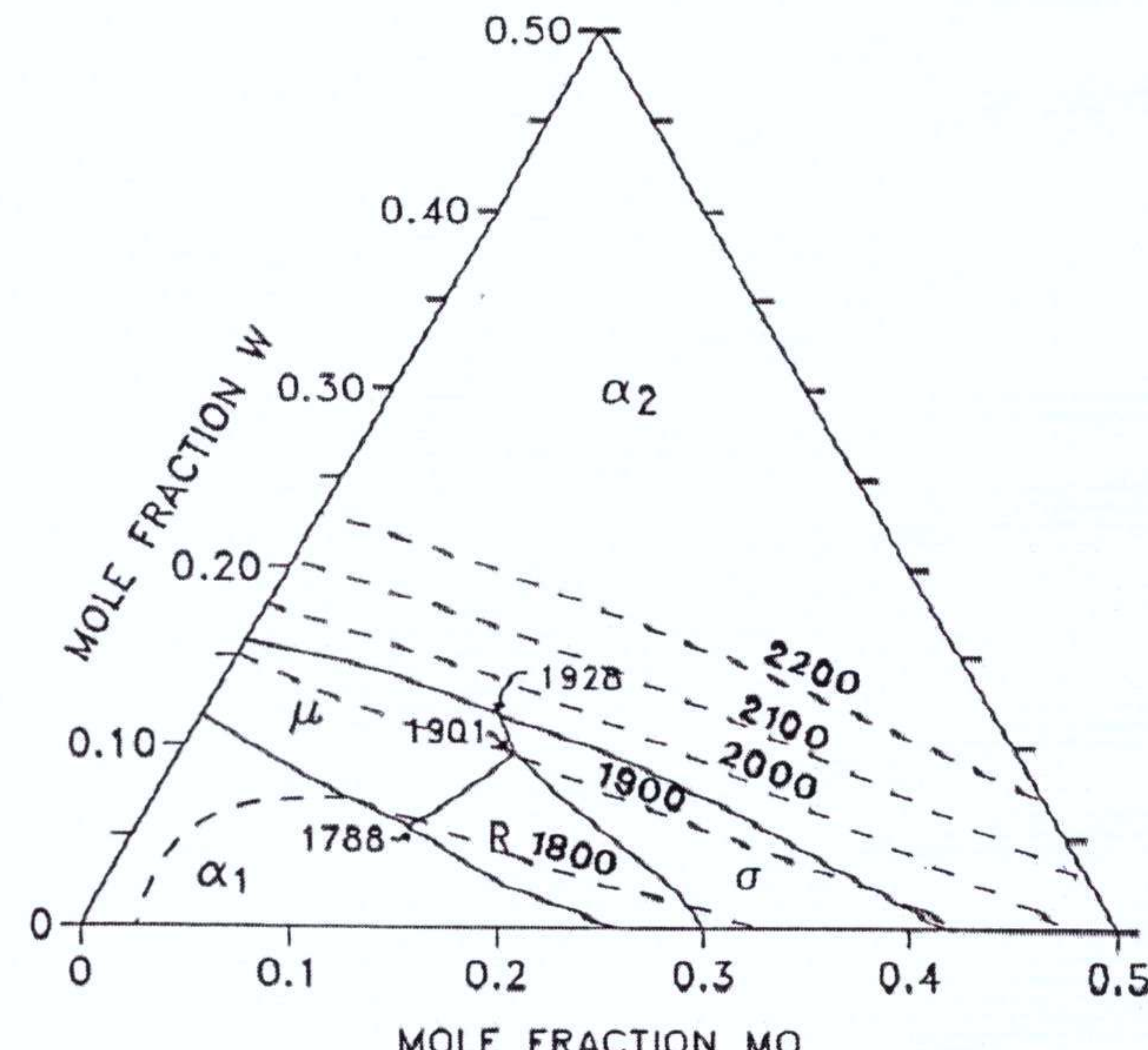


Fig. 14. The calculated projection of the liquidus surface in the Fe-Mo-W system. The full lines show the composition of the liquid phase in simultaneous equilibrium with two solid phases. They separate the various fields of primary crystallization. The dotted lines represent calculated isotherms (in K).

The experimental knowledge of the system outside this region is very sparse. In a recent paper Ishchenko et al.²⁸⁾ presented the results from a brief investigation at 1173, 1273 and 1373 K. They only gave an isothermal section at 1173 K in which the μ phase was shown as a continuous solid solution but the Laves phase as two separate phases with almost no mutual solubility. In a subsequent paper from the same group Meshkov et al.²⁹⁾ presented results from a more elaborate investigation at 1173 K. In that investigation the Laves phase was found to form a continuous solid solution. In order to obtain agreement with this new information a negative interaction energy in the Laves phase had to be introduced. The final description is, as shown in Fig. 13, in good agreement with their data.

No experimental data concerning equilibria involving the liquid phase were found in the literature. As a result no ternary interaction could be evaluated in the liquid phase. It is reasonable, however, to assume that this interaction is negligible since the ternary interaction found in the bcc phase is very small. The calculated projection of the liquidus surface is shown in Fig. 14. The invariant temperatures indicated in this diagram should be regarded as approximate since no experimental data confirming the calculated diagram actually exist. Figure 15 gives a compilation of the calculated three- and four-phase equilibria. All parameters obtained from the present optimization procedure and for the Fe-W sigma phase from the parallel study are given in the Appendix.

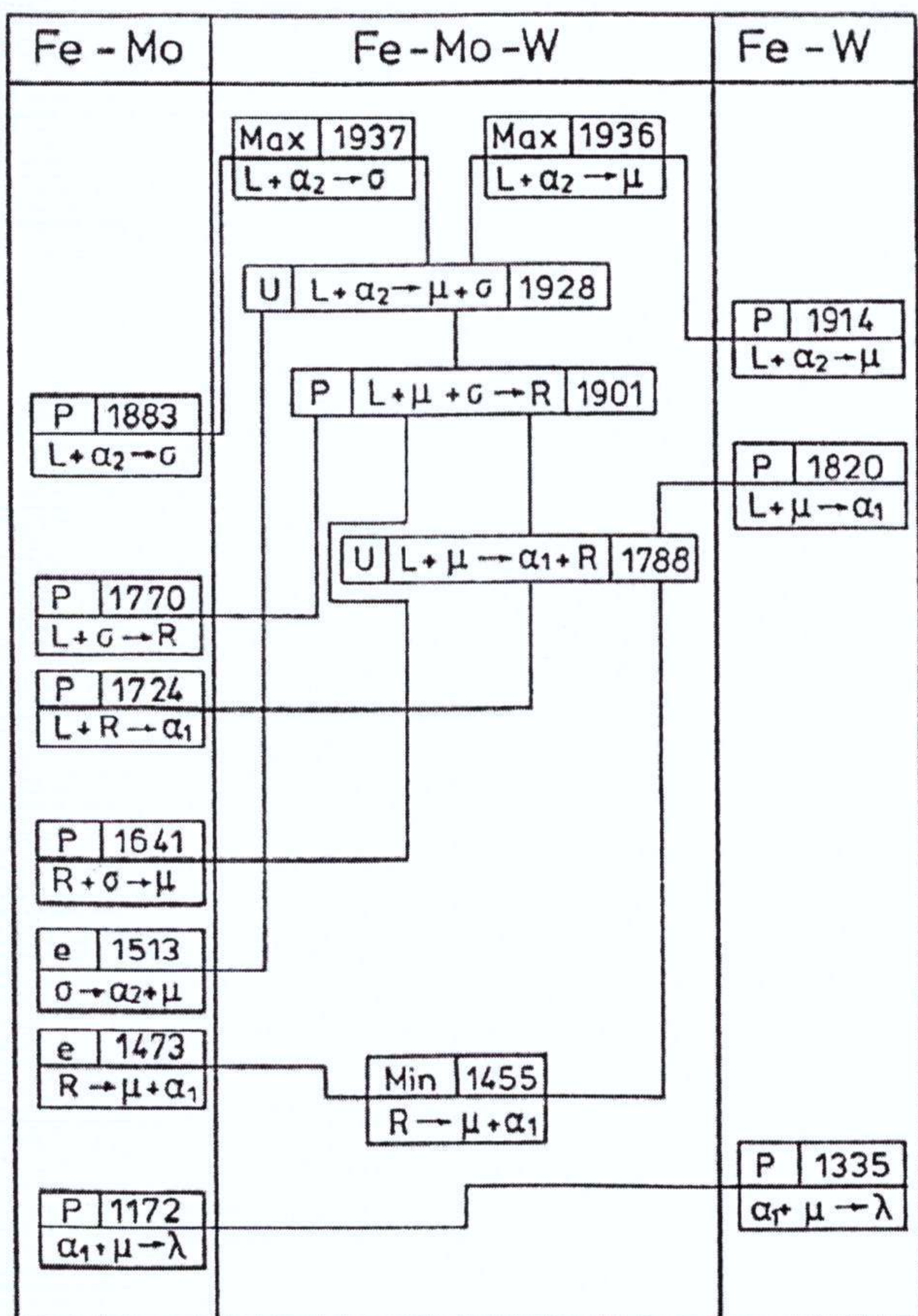


Fig. 15. Compilation of the calculated three- and four-phase equilibria in the Fe-Mo-W system. The temperatures are given in K.

5 Conclusions

New experimental data covering previously uninvestigated regions of the Fe-Mo-W system have been obtained by use of a diffusion couple technique. It has been possible to describe most experimental information by using reasonably simple models, and it was shown that the three-sublattice model adopted for the intermetallic phases can describe all the available experimental data with reasonable accuracy.

6 Appendix 1

Summary of parameters (in SI units and with $R = 8.31451$) obtained in the present work by optimizing the representation of experimental data in the ternary Fe-Mo-W system. Description of the binaries Fe-Mo and Fe-W are given in Refs. ⁹⁾ and ¹³⁾, respectively.

bcc:

Excess model is Redlich-Kister-Muggianu
Constituents: Fe, Mo, W

$$L_{\text{Mo},\text{W}}^{\text{bcc}} = 2000$$

$$L_{\text{Fe},\text{Mo},\text{W}}^{\text{bcc}} = 3000$$

fcc:

Excess model is Redlich-Kister-Muggianu
Constituents: Fe, Mo, W

$$L_{\text{Mo},\text{W}}^{\text{fcc}} = 2000$$

μ -Phase:

3 sublattices, sites 7 : 2 : 4

Excess model is Redlich-Kister-Muggianu

Constituents: Fe : Mo, W : Fe, Mo, W

$${}^0G_{\text{Fe}:\text{Mo}:\text{W}}^{\mu} = 7 {}^0G_{\text{Fe}}^{\text{fcc}} + 2 {}^0G_{\text{Mo}}^{\text{bcc}} + 4 {}^0G_{\text{W}}^{\text{bcc}} - 72000$$

$${}^0G_{\text{Fe}:\text{W}:\text{Mo}}^{\mu} = 7 {}^0G_{\text{Fe}}^{\text{fcc}} + 2 {}^0G_{\text{W}}^{\text{bcc}} + 4 {}^0G_{\text{Mo}}^{\text{bcc}} + 10000$$

R-Phase:

3 sublattices, sites 27 : 14 : 12

Excess model is Redlich-Kister-Muggianu

Constituents: Fe : Mo, W : Fe, Mo, W

$${}^0G_{\text{Fe}:\text{W}:\text{Fe}}^{\text{R}} = 27 {}^0G_{\text{Fe}}^{\text{fcc}} + 14 {}^0G_{\text{W}}^{\text{bcc}} + 12 {}^0G_{\text{Fe}}^{\text{bcc}}$$

$${}^0G_{\text{Fe}:\text{W}:\text{W}}^{\text{R}} = 27 {}^0G_{\text{Fe}}^{\text{fcc}} + 26 {}^0G_{\text{W}}^{\text{bcc}}$$

$${}^0G_{\text{Fe}:\text{Mo}:\text{W}}^{\text{R}} = 27 {}^0G_{\text{Fe}}^{\text{fcc}} + 14 {}^0G_{\text{Mo}}^{\text{bcc}} + 12 {}^0G_{\text{W}}^{\text{bcc}} - 260000$$

$${}^0G_{\text{Fe}:\text{W}:\text{Mo}}^{\text{R}} = 27 {}^0G_{\text{Fe}}^{\text{fcc}} + 14 {}^0G_{\text{W}}^{\text{bcc}} + 12 {}^0G_{\text{Mo}}^{\text{bcc}}$$

σ -Phase:

3 sublattices, sites 8 : 4 : 18

Excess model is Redlich-Kister-Muggianu

Constituents: Fe : Mo, W : Fe, Mo, W

$${}^0G_{\text{Fe}:\text{W}:\text{Fe}}^{\sigma} = 8 {}^0G_{\text{Fe}}^{\text{fcc}} + 4 {}^0G_{\text{W}}^{\text{bcc}} + 18 {}^0G_{\text{Fe}}^{\text{bcc}}$$

$${}^0G_{\text{Fe}:\text{W}:\text{W}}^{\sigma} = 8 {}^0G_{\text{Fe}}^{\text{fcc}} + 22 {}^0G_{\text{W}}^{\text{bcc}} + 200000$$

$${}^0G_{\text{Fe}:\text{Mo}:\text{W}}^{\sigma} = 8 {}^0G_{\text{Fe}}^{\text{fcc}} + 4 {}^0G_{\text{Mo}}^{\text{bcc}} + 18 {}^0G_{\text{W}}^{\text{bcc}} + 28000$$

$${}^0G_{\text{Fe}:\text{W}:\text{Mo}}^{\sigma} = 8 {}^0G_{\text{Fe}}^{\text{fcc}} + 4 {}^0G_{\text{W}}^{\text{bcc}} + 18 {}^0G_{\text{Mo}}^{\text{bcc}}$$

$$L_{\text{Fe}:\text{W}:\text{Fe},\text{W}}^{\sigma} = + 222909$$

$$L_{\text{Fe}:\text{Mo}:\text{Fe},\text{W}}^{\sigma} = + 222909$$

$$L_{\text{Fe}:\text{W}:\text{Fe},\text{Mo}}^{\sigma} = + 222909$$

Laves-Phase:

2 sublattices, sites 2 : 1

Excess model is Redlich-Kister

Constituents: Fe : Mo, W

$$L_{\text{Fe}:\text{Mo},\text{W}}^{\text{laves}} = - 7500$$

The author wishes to express his gratitude to Prof. Mats Hillert for useful advice, constructive criticism and for the help received during the preparation of this paper. I also wish to thank Mr. Nils Lange for the help received during the experimental work and Dr. Björn Uhrenius at Sandvik Hard Materials Research Center for supplying the alloys.

All phase diagrams in this report have been calculated with a computer program Thermo-Calc developed by Dr. Bo Sundman, Dr. Bo Jansson and Jan-Olaf Andersson at the Division of Physical Metallurgy³⁰⁾. The work was supported by the Swedish National Board for Technical Development.

Literature

- 1) G. V. RAYNOR and V. G. RIVLIN, Int. Metals Rev. **4** (1981) 224-226.
- 2) G. KIRCHNER, H. HARVIG, and B. UHRENIUS, Metall. Trans. **4** (1973) 1059-1067.
- 3) A. FERNANDEZ GUILLERMET, Bulletin of Alloy Phase Diagram **3** (1982) 359-367.
- 4) A. FERNANDEZ GUILLERMET, personal communication.
- 5) B. SUNDMAN and J. ÅGREN, J. Phys. Chem. Solids **42** (1981) 297-301.
- 6) G. INDEN, Proj. Meeting Calphad V (1976) III. 4-1.
- 7) M. HILLERT and M. JARL, Calphad **2** (1978) 227-238.
- 8) J.-O. ANDERSSON and B. SUNDMAN, Trita-Mac-0270, Div. Phys. Metall., Royal Inst. Techn. Stockholm, Sweden (1986).
- 9) J.-O. ANDERSSON, Trita-Mac-0322, Div. Phys. Metall., Royal Inst. Techn. Stockholm, Sweden (1986).
- 10) P. GUSTAFSON, Trita-Mac-0320, Div. Phys. Metall., Royal Inst. Techn. Stockholm, Sweden (1986).
- 11) K. FRISK, personal communication.
- 12) J.-O. ANDERSSON and P. GUSTAFSON, Calphad **7** (1983) 317-326.
- 13) P. GUSTAFSON, Metall. Trans. **18A** (1987) 175-188.
- 14) J.-O. ANDERSSON, A. FERNANDEZ GUILLERMET, M. HILLERT, B. JANSSON, and B. SUNDMAN, Acta Metall. **34** (1986) 437-445.
- 15) P. GUSTAFSON, Trita-Mac-0342, Div. Phys. Metall., Royal Inst. Techn. Stockholm, Sweden (1987). Accepted for publication in Met. Trans. A.
- 16) A. FERNANDEZ GUILLERMET and P. GUSTAFSON, High Temp. High Press. **16** (1985) 591-610.
- 17) A. FERNANDEZ GUILLERMET, Int. J. Thermophys. **6** (1985) 367-393.
- 18) P. GUSTAFSON, Int. J. Thermophys. **6** (1985) 395-409.
- 19) B. JANSSON, Trita-Mac-0234, Div. Phys. Metall., Royal Inst. Techn. Stockholm, Sweden (1984).
- 20) B. JANSSON, Internal report D57, Div. Phys. Metall., Royal Inst. Techn. Stockholm, Sweden (1984).
- 21) S. V. NAGENDER NAIDU, A. M. SRIRAMAMURTHY, and P. RAMA RAO, Bulletin of Alloy Phase Diagram **5** (1984) 177-180.
- 22) L. KAUFMAN and H. BERNSTEIN, in Computer Calculation of Phase Diagrams, Academic Press, New York (1970) 74-91 and 238.
- 23) L. BREWER and R. H. LAMOREAUX, Molybdenum: Physico-Chemical Properties of its Compounds and Alloys, Atom. Energy Rev. Spec. Issue 7 : 18 (1980) 149.
- 24) F. A. FAHRENWALD, Trans. AIME **56** (1917) 612-619.
- 25) Z. JEFFRIES, Trans. AIME **56** (1917) 600-611.
- 26) V. V. BARON, E. M. SAVITSKII, and K. N. IVANOVA, Russ. Met. Fuels (2) (1962) 87-97.
- 27) E. RUDY, "Compendium of Phase Diagram Data", Air Force Materials Laboratory, Wright-Patterson Air Force Base, OH, Rep. No. AFML-TR-65-2, Part V, 154-156 (May 1969).
- 28) T. V. ISHCHEKO, L. L. MESHKOV, and Y. M. SOKOLOVSKAYA, J. Less-Common Met. **97** (2) (1984) 145-150.
- 29) L. L. MESHKOV, S. N. NESTERNENKO, and T. V. ISHCHEKO, Izvest. Akad. Nauk SSSR, Met. **2** (1985) 205-208.
- 30) B. SUNDMAN, B. JANSSON, and J.-O. ANDERSSON, Calphad **9** (1985) 153-190.

(Eingegangen am 21. November 1987)

subito copyright regulations



Copies of articles ordered through subito and utilized by the users are subject to copyright regulations. By registering with subito, the user commits to observing these regulations, most notably that the copies are for personal use only and not to be disclosed to third parties. They may not be used for resale, reprinting, systematic distribution, emailing, web hosting, including institutional repositories/archives or for any other commercial purpose without the permission of the publisher.

Should delivery be made by e-mail or FTP the copy may only be printed once, and the file must be permanently deleted afterwards.

The copy has to bear a watermark featuring a copyright notice. The watermark applied by subito e.V. must not be removed.